Fast intramolecular proton transfer in 2-(hydroxyaminomethylidene)-indan-1,3-dione

ARTICLE *in* JOURNAL OF MOLECULAR STRUCTURE THEOCHEM · APRIL 2005

Impact Factor: 1.37 · DOI: 10.1016/j.theochem.2005.01.030

ELSEVIER

Journal of Molecular Structure: THEOCHEM 719 (2005) 169–175

THEO CHEM

www.elsevier.com/locate/theochem

Fast intramolecular proton transfer in 2-(hydroxyaminomethylidene)-indan-1,3-dione

Venelin Enchev[a,*], Isaac Abrahams[b], Silvia Angelova[a], Galya Ivanova[a]

[a]*Institute of Organic Chemistry, Bulgarian Academy of Sciences, Acad G. Bontchev Str. Bl. 9, 1113 Sofia, Bulgaria*
[b]*Centre for Materials Research, Department of Chemistry, Queen Mary, University of London, Mile End Road, London E1 4NS, UK*

Received 6 January 2005; accepted 21 January 2005

Abstract

The structure of 2-carboxamide-indan-1,3-dione was investigated in gas phase, solution and solid states using a combination of quantum-chemical calculations, NMR spectroscopy and X-ray crystallography. Quantum-chemical calculations indicate that two tautomeric forms, 2-(hydroxyaminomethylidene)-indan-1,3-dione (**A**) and 2-carboamide-1-hydroxy-3-oxo-indan (**B**), are likely to coexist, with fast intramolecular proton transfer between them. The calculations were carried out at HF and MP2 level of theory using 6-31G** and 6-311G** basis sets. The energy barrier of the intramolecular proton transfer reaction was calculated as 2.30 kcal mol^{-1} at the MP4/6-311G**//MP2/6-311G** level. ^{1}H and ^{13}C NMR spectra are consistent with the coexistence of tautomers **A** and **B** in solution, while X-ray crystallography suggests the exclusive presence of tautomer **A** in the solid state.

Keywords: 2-Carboxamide-indan-1,3-dione; 2-(Hydroxyaminomethylidene)-indan-1,3-dione; Tautomerism; Ab initio; NMR; Crystal structure

1. Introduction

The two-substituted 1,3-indandiones are biologically active compounds, which are applied as anticoagulants, inhibitors of auto-oxidation processes in liquid phases and stabilizing agents for polymers [1]. These compounds can exist in at least in three tautomeric forms [2] and in five tautomeric forms if the substituent at position 2 is included in the process of tautomerisation (Fig. 1). Recently, we reported experimental and theoretical studies of excited state intramolecular proton transfer in 2-acetyl-indan-1,3-dione (**2AID**) [3,4]. It was found that **2AID** exists as the 2-(1-hydroxyethylidene)-indan-1,3-dione tautomer [3,5]. The syntheses of its analogue 1,3-dioxo-2-indancarboxamide was reported by Horton and Murdock [6] over 40 years ago, but to date the structure of the compound has not been elucidated. The compound exists in the solid state as yellow–orange needles, which sinter from 180 to 220 °C [6].

In this work, we present the results of ab initio calculations of the energy difference between the possible tautomers of 1,3-dioxo-2-indancarboxamide and of the barrier height for conversion between the two most stable tautomers. These results are compared with those from NMR spectroscopy and X-ray crystallography.

2. Computational and experimental details

2.1. Quantum chemical calculations

The calculations were carried out using the PC GAMESS version [7] of the GAMESS (US) quantum chemistry package [8]. The geometries of all possible tautomeric forms of the title compound, shown in Fig. 1, were located at HF/3-21G and HF/6-31G** levels. Selected structures were re-optimized at a second order Møller–Plesset perturbation level of theory (MP2) using the 6-31G** and 6-311G** basis sets. The transition structure for tautomeric conversion between the two most stable tautomers was located at MP2/6-31G** and MP2/6-311G** levels. The default gradient convergence threshold (1×10^{-4} ha $Bohr^{-1}$) was used. Frequency calculations at the same level of theory were carried out to determine whether the optimized structures

* Corresponding author. Tel.: +359 2 9606197; fax: +359 2 8700225.
E-mail address: venelin@orgchm.bas.bg (V. Enchev).

0166-1280/$ - see front matter © 2005 Elsevier B.V. All rights reserved.
doi:10.1016/j.theochem.2005.01.030

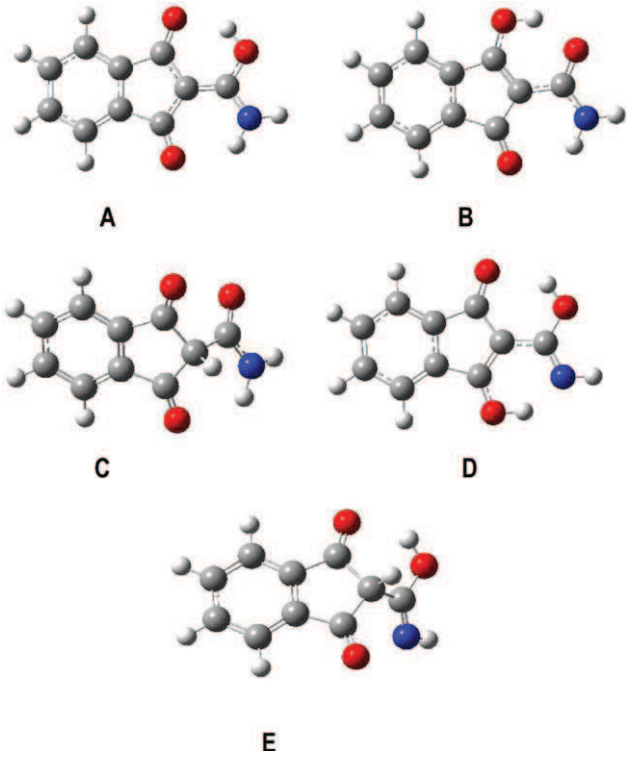

Fig. 1. Tautomeric forms of 2-(hydroxyaminomethylidene)-indan-1,3-dione.

were local minima or transition states (TSs) on the potential energy surface and to estimate thermal corrections. To obtain accurate energies, single-point calculations at MP4/6-31G**//MP2/6-31G** and MP4/6-311G**//MP2/6-311G** levels of theory were performed. Unscaled ZPE corrections were included in the relative energy values. Force field calculations for the two most stable tautomers in which labile hydroxyl and amino protons were substituted by deuterium (D) and tritium (T), were carried out.

The values of Gibbs free energies were calculated using the formula $\Delta G = \Delta H - T\Delta S$. The classical rate constants at 298.15 K were calculated using the Eyring equation, $k = (k_B T/h)\exp(-\Delta G^{\#}/RT)$, where k_B and h are the Boltzmann and Planck constants, respectively.

To estimate the solvent effect (chloroform and DMSO) on the relative stabilities of the tautomers, the static isodensity polarized continuum model (IPCM) [9] as implemented in the GAUSSIAN 03 [10] suite of programs was applied at the MP2/6-31G** level for the geometries optimized at the same level of theory (IPCM/MP2/6-31G**//MP2/6-31G**).

The ^{13}C NMR chemical shieldings of the tautomeric forms, 2-(hydroxyaminomethylidene)-indan-1,3-dione and 2-carboamide-1-hydroxy-3-oxo-indan, were calculated at the HF/6-31+G* level using the GIAO [11,12] approach and HF/6-31G**, MP2/6-31G** and MP2/6-311G** optimized geometry. For these calculations GAUSSIAN 03 was used. In order to compare with experiment, the calculated absolute shieldings were transformed to chemical shifts using the reference compound tetramethylsilane, $Si(CH_3)_4$, (TMS): $\delta = \delta_{calc}(TMS) - \delta_{calc}$. Both $\delta_{calc}(TMS)$ and δ_{calc} were evaluated at the same computational level.

2.2. Synthesis of 1,3-dioxo-2-indanecarboxamide

1,3-Dioxo-2-indancarboxamide was synthesized according to Ref. [6]. Single crystals for X-ray crystallographic measurements were re-crystallized from ethanol.

2.3. NMR measurements

NMR spectra were recorded on a Bruker DRX-250 spectrometer, operating at 250.13 for ^1H and 62.9 MHz for ^{13}C, using a 5 mm dual probe head. The chemical shifts are referenced to TMS in $CDCl_3$, 3-(trimethylsilyl)propionic acid-d_4 sodium salt (TSPA) in D_2O and to the solvent signal in ethanol-d_6 and DMSO-d_6. The measurements were carried out at ambient temperature (ca. 300 K), in solvents $CDCl_3$, ethanol-d_6, DMSO-d_6 and D_2O. Sample concentrations of 0.01–0.05 M for ^1H and saturated solutions for ^{13}C NMR spectra were used. Typical conditions for the 1D experiment were: 30° pulses, 1 s relaxation delay, 16 K time domain points, zero-filled to 32 K. Hard pulses with 90° pulse widths of 11.4 μs for ^1H and 6.0 μs for ^{13}C at a power level of 3 dB below the maximum output were used. Distortionless enhancement by polarisation transfer (DEPT) spectra were obtained under the same conditions as the ^{13}C-NMR spectra, and $\tau = (2^1J_{CH})^{-1} = 3.45$ ms was used.

The deuteration of 2-(hydroxyaminomethylidene)-indan-1,3-dione was achieved by dissolving of 20 mg of the compound in 1 ml chloroform and stirring with 0.3 ml D_2O. The organic phase was separated and treated with another portion of 0.3 ml D_2O. The procedure was repeated to complete deuteration, and was monitored by ^1H NMR.

2.4. X-ray crystallography

Single crystal X-ray diffraction data were collected at 120 K using a Nonius Kappa CCD area detector diffractometer mounted at the window of molybdenum rotating anode generator (50 kV, 90 mA, $\lambda = 0.71069$ Å). The crystal-to-detector distance was 30 mm and ϕ and Ω scans (2.0° increments, 12 s exposure time) were carried out to fill the Ewald sphere. Data collection and processing were carried out using COLLECT [13], DENZO [14] and maXus [15], with empirical absorption correction applied using SADABS [16]. All crystals showed a number of twin components related by small rotations about 0 1 0. For structure determination data were deconvoluted into four batches containing reflections from individual twin components. Due to this problem, all 0 k 0 reflections were absent from the data and space group confirmation was carried out using X-ray powder diffraction data.

Table 1
Crystal and refinement parameters for 2-(hydroxyaminomethylidene)-indan-1,3-dione

Empirical formula	$C_{10}H_7NO_3$
Formula weight	189.17
Temperature	120(2) K
Wavelength	0.71073 Å
Crystal system	Monoclinic
Space group	$P2_1/c$
Unit cell dimensions	$a=7.063(2)$, $b=9.612(3)$, $c=12.332(5)$ Å, $\beta=105.5(2)°$
Volume	806.6(5) Å^3
Z	4
Density (calculated)	1.558 mg m^{-3}
Absorption coefficient	0.117 mm^{-1}
$F(000)$	392
Crystal size	$0.06\times0.06\times0.03$ mm^3
Reflections collected	5325
Independent reflections	1453 [R(int)=0.2024]
Data/restraints/parameters	1453/0/132
Goodness-of-fit on F^2	1.067
Final R indices [$I>2\sigma(I)$]	$R_1=0.1366$, $wR_2=0.3040$
R indices (all data)	$R_1=0.2783$, $wR_2=0.3586$
Largest diff. peak and hole	0.506 and −0.381 e Å^{-3}

The structure was solved by direct methods using SHELXS-97 [17] in the monoclinic space group $P2_1/c$ and refined anisotropically (non-hydrogen atoms) by full-matrix least-squares on F^2 using the SHELXL-97 program [17]. The ring H atoms and those on N1 were calculated geometrically and refined with an atom-riding model. H5 was located in the difference Fourier map and refined independently. The twinning problem described above and the small crystal size meant that the data quality prohibited an unconstrained refinement of the H-atoms and is reflected in the high refinement R-factors. The programs ORTEP-3 [18] and Platon [19] were used for drawing the molecule. WINGX [20] was used to prepare material for publication. Crystal data and refinement details are given in Table 1. The crystal structure has been deposited at the Cambridge Crystallographic Data Centre and allocated the deposition number CCDC 260733.

3. Results and discussion

2-Carboxamide-indan-1,3-dione can theoretically exist in 5 tautomeric forms, **A**–**E**, shown in Fig. 1. In the original work of Horton and Murdock [6], the compound is indicated as tautomer **C**. However, our ab initio quantum chemical calculations at different levels of theory predict 2-(hydroxyaminomethylidene)-indan-1,3-dione (tautomer **A**) as most stable. The next in energy is 2-carboamide-1-hydroxy-3-oxo-indan (tautomer **B**) (Table 2). At the HF level of calculation, the difference between both tautomers is 1.95–4.5 kcal mol^{-1} depending on the basis set used. Improving basis set quality leads to a decrease in this difference. When electron correlation and ZPE are taken into account in the calculations, the energy difference between **A** and **B** tautomers becomes smaller than 0.5 kcal mol^{-1}. At the MP4/6-31G**//MP2/6-31G**+ZPE level, the difference is only 0.28 kcal mol^{-1} and these tautomers can be considered to be isoenergetic.

Table 2
HF and MP2 calculated relative stabilities (kcal mol^{-1}) for the tautomers of 2-(hydroxy-aminomethylidene)-indan-1,3-dione shown in Fig. 1

Method	Tautomers				
	A	**B**	**C**	**D**	**E**
HF/3-21G	0.00	4.82	14.61	24.22	35.88
HF/3-21G+ZPE	0.00	4.49	13.44	23.11	34.08
HF/6-31G**	0.00	2.08	7.98	17.27	24.49
HF/6-31G**+ZPE	0.00	1.95	7.15	17.51	23.87
MP2/6-31G**//HF/6-31G**+ZPE	0.00	0.76	5.10	14.35	21.07
MP2/6-31G**	0.00	0.93	5.28	13.66	
MP2/6-31G**+ZPE	0.00	0.47			
MP4/6-31G**//MP2/6-31G**+ZPE	0.00	0.28			
MP2/6-311G**	0.00	0.92			
MP2/6-311G**+ZPE	0.00	0.80			
MP4/6-311G**//MP2/6-311G**+ZPE	0.00	0.65			
IPCM/MP2/6-31G**//MP2/6-31G**+ZPE					
Solvent $CHCl_3$	0.00	0.04			
Solvent DMSO	0.38	0.00			

At HF/3-21G, HF/6-31G** and MP2/6-31G**//HF/6-31G** levels of theory, the species **D** and **E** are more than 14 kcal mol^{-1} less stable than tautomer **A** and are therefore not considered further in our analysis. At MP2/6-31G**//HF/6-31G**+ZPE level, tautomer **C** was found to be 5.10 kcal mol^{-1} higher in energy than **A**. The calculations at MP2/6-31G** level did not change this difference substantially (Table 2). Taking into account the small energy difference between **A** and **B**, the tautomer **C** (2-carboxamide-indan-1,3-dione) might be also eliminated from consideration. This suggestion was confirmed by ^{1}H and DEPT-135 experiments in solvents $CDCl_3$ and DMSO-d_6. The absence of a proton at position C9 confirms the exclusion of tautomer **C**. Furthermore, the presence of two NH proton resonances (at 8.30 and 9.08 ppm in DMSO-d_6) is consistent with the non-existence of tautomers **D** and **E**. The downfield shift of one of these NH resonances is indicative of intramolecular H-bonding (O2···H6).

The quality of the basis set and level of calculations substantially influences the calculated barrier of tautomerisation (Table 2). The inclusion of high-order correlation contributions increases the barrier height. However, in this case, the calculated barrier of activation is too low at all levels of theory. For example, at the MP4/6-311G**//MP2/6-311G** level, the activation barrier of intramolecular proton transfer reaction was calculated to be 2.13 kcal mol^{-1}. The substitution of the labile protons H5, H6 and H7 with deuterium and tritium leads to increases in the activation barriers, but the predicted values at 298.15 K are also low (Table 3). Table 4 shows the total energy and ZPE values of the isotopically substituted tautomers used in the calculation of enthalpy and free energy values presented in Table 3.

Table 3
Calculated relative stabilities and energy barriers $\Delta H_0^{\#}$ and $\Delta G_{298}^{\#}$ (in kcal mol^{-1}) for the tautomers **A** and **B** of 2-(hydroxy-aminomethylidene)-indan-1,3-dione

Computational level	Isotope	ΔH_0	ΔG_{298}	$\Delta H_0^{\#}$	$\Delta G_{298}^{\#}$	$\nu^{\#}$	k
MP2/6-31G**	H	0.47	0.18	1.29	1.49	1162*i*	5.02×10^{11}
	D	0.54	0.24	2.21	2.29	862*i*	1.30×10^{11}
	T	0.57	0.27	2.47	2.67	723*i*	6.85×10^{10}
MP4/6-31G**//	H	0.28	−0.01	2.64	2.79		5.60×10^{10}
MP2/6-31G**	D	0.35	0.05	3.46	3.63		1.36×10^{10}
	T	0.38	0.08	3.81	4.01		7.14×10^{9}
MP4/6-	H	0.65	0.61	2.13	1.80	1119*i*	2.98×10^{11}
311G**//MP2/	D	0.32	0.07	2.94	2.64	834*i*	7.21×10^{10}
6-311G**	T	0.35	0.10	3.28	3.01	701*i*	3.86×10^{10}
IPCM/MP2/6-31G**							
$CHCl_3$	H	0.04	−0.26	2.04	2.44		1.01×10^{11}
DMSO	H	−0.38	−0.68	2.86	3.29		2.41×10^{10}

Imaginary frequencies $\nu^{\#}$ are in cm^{-1}. The rate constants are in s^{-1}.

The rate constant of the tautomerisation reaction, calculated by the Eyring equation is found to be in the order of $1\times10^{10}-1\times10^{11}$ s^{-1}. This suggests that the proton transfer reaction is extremely fast. Structural parameters for this TS are given in Table 5. Substantial changes are observed in the moiety in which proton transfer occurs. The C7–O3 and C10–O1 bonds become almost equal (1.28 Å), while the C8–C9 bond length decreases and the C9–C10 bond length increases in comparison with those in tautomer **A**. The migrating proton is located approximately centrally between O1 and O3 atoms.

The gas-phase and IPCM calculated relative stabilities in solvents $CHCl_3$ ($\varepsilon=4.9$) and DMSO ($\varepsilon=46.7$) of tautomers **A** and **B** obtained at MP2/6-31G** level, are presented in Table 3. In $CHCl_3$, tautomeric form **A** is also found to be more stable. The enthalpy difference at 0 K (ΔH_0) between **A** and **B** is only 0.04 kcal mol^{-1}. In DMSO, tautomer **B** is more stable. In this case, ΔH_0 is calculated to be 0.38 kcal mol^{-1}. This is in agreement with the expectation that polar species are stabilized more in a polar solvent than in a non-polar one.

The MP2/6-31G** calculated Gibbs free energy differences of **A** and **B** in solution are presented in Table 3. In both solvents, tautomer **B** is preferred. The difference in the Gibbs free energies in $CHCl_3$ is 0.26 kcal mol^{-1}, while in DMSO is 0.68 kcal mol^{-1}. On the basis of these differences, the relative populations of tautomers **A** and **B** were calculated to be **A**:**B** = 39.2:60.8% and **A**:**B** = 31.7:68.3% in $CHCl_3$ and DMSO, respectively. It was found that the activation barrier in solution increased by 0.95 and 1.80 kcal mol^{-1} in $CHCl_3$ and DMSO, respectively, in comparison to the isolated molecule.

In order to study the equilibrium between the structures **A** and **B** in solution, ^{1}H and ^{13}C NMR spectra were recorded in solvents of differing polarities. In the ^{13}C spectra, one set of narrow signals was observed in all solvents used and were assigned to six unique carbon environments as recorded in Table 6. All spectra showed chemical shift equivalences of C1/C4, C2/C3, C5/C6 and C7/C8 carbon pairs. In order to explain this it is helpful to compare the observed chemical shift values with those calculated for the two lowest energy tautomers, **A** and **B**, in $CHCl_3$ and DMSO solutions (Table 6).

Table 4
Total energy, E_T and zero-point energy, ZPE (a.u.) for isotopic substituted tautomers **A**, **B** and transition state (TS) of 2-(hydroxy-aminomethylidene)-indan-1,3-dione calculated at different computational levels

Computational level	Species	E_T	ZPE		
			H	D	T
MP2/6-31G**	**A**	−663.838003	0.155374	0.144959	0.140441
	B	−663.836525	0.154651	0.144341	0.139873
	TS	−663.831665	0.151107	0.142004	0.138045
MP4/6-31G**//MP2/	**A**	−663.883696			
6-31G**	**B**	−663.882523			
	TS	−663.875227			
MP2/6-311G**	**A**	−664.121898	0.153176	0.142887	0.138426
	B	−664.120431	0.152488	0.142275	0.137854
	TS	−664.116163	0.148645	0.139644	0.135730
MP4/6-311G**//MP2/	**A**	−664.153561			
6-311G**	**B**	−664.152432			
	TS	−664.145631			

Table 5
MP2/6-31G** and MP2/6-311G** calculated distances (Å), bond angles (degrees) and dipole moments (*D*) for tautomers **A**, **B** and transition state of 2-(hydroxyaminomethylidene)-indan-1,3-dione

Parameter	Tautomer **A**			Tautomer **B**		Transition state	
	X-ray	6-31G**	6-311G**	6-31G**	6-311G**	6-31G**	6-311G**
Distances							
C1–C2	1.417(14)	1.4005	1.4022	1.4040	1.4058	1.4026	1.4044
C2–C3	1.383(12)	1.4016	1.4036	1.3983	1.4003	1.3994	1.4014
C3–C4	1.450(16)	1.4007	1.4024	1.4044	1.4063	1.4031	1.4050
C4–C5	1.337(14)	1.3884	1.3904	1.3839	1.3858	1.3854	1.3874
C5–C6	1.406(11)	1.4050	1.4054	1.4055	1.4059	1.4078	1.4078
C6–C1	1.380(14)	1.3888	1.3908	1.3866	1.3887	1.3874	1.3894
C6–C8	1.492(13)	1.4940	1.4966	1.4747	1.4762	1.4817	1.4835
C5–C7	1.538(14)	1.5015	1.5050	1.5055	1.5092	1.5091	1.5128
C7–C9	1.410(11)	1.4466	1.4502	1.4669	1.4704	1.4501	1.4539
C8–C9	1.403(13)	1.4368	1.4397	1.3725	1.3741	1.3970	1.3992
C9–C10	1.445(15)	1.3897	1.3912	1.4573	1.4608	1.4216	1.4249
C10–N1	1.270(11)	1.3328	1.3354	1.3491	1.3526	1.3379	1.3401
C8–O2	1.234(9)	1.2418	1.2307	1.2354	1.2243	1.2376	1.2266
C7–O3	1.247(10)	1.2506	1.2405	1.3209	1.3139	1.2854	1.2767
C10–O1	1.300(11)	1.3285	1.3212	1.2542	1.2436	1.2876	1.2782
O1–H5	0.95(8)	0.9969	0.9947	1.7342	1.7196	1.2318	1.2257
O3–H5	1.90(10)	1.7718	1.7469	1.0021	0.9991	1.2116	1.2026
O3–O1	2.70(1)	2.6835	2.6650	2.6349	2.6229	2.4039	2.3930
N1–H7	0.86	1.0051	1.0077	1.0054	1.0085	1.0054	1.0078
N1–H6	0.86	1.0126	1.0143	1.0094	1.0113	1.0097	1.0115
O2–H6	2.31(1)	2.1507	2.1757	2.2049	2.2275	2.3371	2.3650
O2–N1	2.94(1)	2.9107	2.9351	2.9720	2.9932	3.0684	3.0946
Bond angles							
C1–C2–C3	120.7(10)	121.0	121.0	121.2	121.2	121.1	121.1
C2–C3–C4	120.0(9)	121.0	121.0	120.9	120.8	121.0	120.9
C3–C4–C5	116.2(8)	117.8	117.8	117.7	117.8	117.9	117.9
C4–C5–C6	125.7(10)	121.1	121.1	121.3	121.2	121.0	120.9
C5–C6–C1	117.8(8)	121.4	121.4	121.5	121.5	121.5	121.6
C6–C1–C2	119.5(7)	117.7	117.7	117.4	117.4	117.5	117.5
C5–C6–C8	110.3(8)	108.5	108.6	107.0	107.0	107.1	107.2
C6–C5–C7	105.0(7)	109.1	109.3	108.2	108.2	109.0	109.1
C5–C7–C9	107.1(7)	105.3	105.1	105.7	105.5	104.9	104.7
C6–C8–C9	106.3(7)	108.2	108.1	110.8	110.6	108.7	108.7
C7–C9–C8	111.3(9)	110.7	110.8	108.5	108.6	110.2	110.2
C9–C8–O2	129.7(9)	128.0	128.2	127.7	127.9	128.2	128.5
C9–C7–O3	129.0(9)	128.5	128.5	128.5	126.5	123.8	123.8
C8–C9–C10	126.6(7)	121.9	121.4	121.0	120.5	117.5	117.0
C9–C10–N1	121.9(8)	122.2	122.3	116.3	116.3	120.2	120.2
C9–C10–O1	118.1(7)	121.0	120.8	120.1	120.1	118.4	118.4
C10–O1–H5	115(6)	105.7	105.0	101.5	101.6	102.7	102.4
C7–O3–H5	94(3)	94.4	94.3	103.4	103.0	98.2	97.8
C10–N1–H7	120.0	120.3	119.2	119.0	118.0	119.9	119.2
C10–N1–H6	120.0	116.9	116.2	119.4	118.5	118.2	117.7
Dipole moment		0.96	1.10	2.06	1.90	1.17	1.05

From the calculations discussed above tautomers **A** and **B** are predicted to coexist in solution adding to the difficulty of direct comparison between experimental and calculated chemical shift values. On the basis of the IPCM calculated relative populations of tautomers **A** and **B** in $CHCl_3$ and DMSO discussed above, average ^{13}C chemical shifts in these solvents were calculated and compared to the experimentally observed values. The average differences between the average chemical shifts obtained by MP2/6-31G** optimized geometry and the corresponding experimentally observed values showed relatively low average deviations ($\Delta\delta$) of 1.39 and 2.09 ppm in $CHCl_3$ and DMSO. The experimental results are therefore consistent with a mixture of tautomers **A** and **B** in solution.

The calculated structural parameters of tautomers **A** and **B** are listed in Table 5. It should be noted that the MP2/6-31G** calculations predict slightly longer C–C and C–N bond lengths and shorter C–O and O–H bond lengths and O–H···O distances than the MP2/6-311G** calculations.

Table 5 also shows bond lengths and angles derived from the crystal structure analysis. The X-ray data were modelled successfully on the structure of tautomer **A**. However, since

Table 6
Experimental and GIAO ^{13}C chemical shifts (ppm) calculated at HF/6-31+G* level of theory of 2-(hydroxyaminomethylidene)-indan-1,3-dione

Atom	Experimental				GIAO HF/6-31+G*//MP2/6-31G**			
	$CDCl_3$	Ethanol-d_6	D_2O	DMSO-d_6	**A**	**B**	**A**:**B**[a]	**A**:**B**[b]
C1	121.1	121.9	123.0	120.9	124.9	125.5	125.3	125.3
C2	132.8	133.9	135.6	133.1	133.9	134.3	134.1	134.2
C3	132.8	133.9	135.6	133.1	133.0	132.8	132.9	132.9
C4	121.1	121.9	123.0	120.9	125.0	124.1	124.5	124.4
C5	138.5	139.4	140.8	138.2	139.7	136.2	137.6	137.4
C6	138.5	139.4	140.8	138.2	141.3	136.3	138.3	137.9
C7	192.5	193.5	197.4	191.1	200.0	192.9	195.7	195.1
C8	192.5	193.5	197.4	191.1	194.9	195.2	195.1	195.1
C9	95.1	93.5	95.9	92.2	85.9	96.1	92.1	92.9
C10	168.7	169.4	170.2	167.5	171.4	172.4	172.0	172.1

For numbering of the atoms, see Fig. 2. Geometries of tautomers **A** and **B** are optimized at MP2/6-31G** computational level.
[a] **A**:**B**=39.2:60.8% (solvent $CHCl_3$).
[b] **A**:**B**=31.7:68.3% (solvent DMSO).

most of the H-atoms were geometrically calculated and refined using an atom-riding model, only the non-H atom positions can be treated with any degree of certainty and one must therefore consider all the possible tautomers before a conclusion regarding the true identity of that in the crystal structure can be made. In the solid state, the molecule is clearly planar (Fig. 2), this therefore eliminates tautomers **C** and **E** from consideration. Only the OH hydrogen atom, H(5), was unambiguously identified in the difference Fourier map and refined independently. This would appear to be consistent with tautomers **A** and **D**. However, on this basis one cannot totally exclude tautomer **B**, as a rotation about the C9–C10 bond would lead to an almost indistinguishable situation since O and N exhibit very similar X-ray scattering. The C8–O2 and C7–O3 bond lengths of 1.234 and 1.247 Å, respectively, appear to be consistent with both being carboxyl groups rather than one of them being an alcohol. Indeed, the calculated values for these two bond lengths for tautomer **B** in Table 5 show a difference of around 0.09 Å and a similar difference would be expected in tautomer **D**. One can therefore conclude that the crystal structure suggests the exclusive presence of tautomer **A** in the solid state.

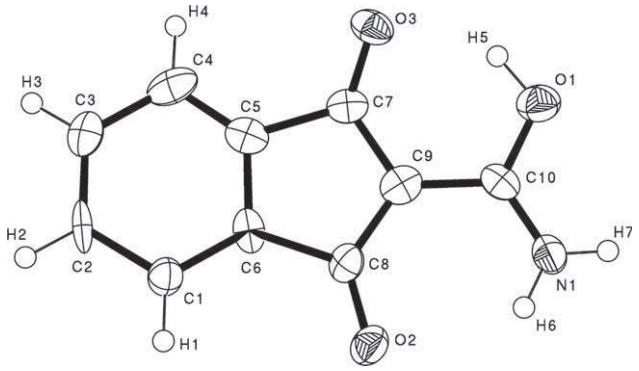

Fig. 2. Thermal ellipsoid plot (30% probability) of crystal structure of 2-(hydroxyaminomethylidene)-indan-1,3-dione.

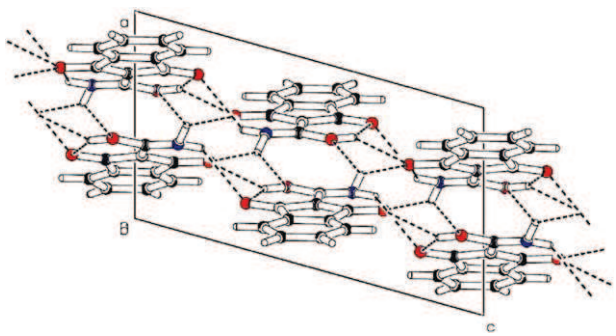

Fig. 3. Projection down *b*-axis of crystal structure of 2-(hydroxyaminomethylidene)-indan-1,3-dione. Hydrogen bonds are indicated by dashed lines.

In the solid state, the planar molecules of 2-(hydroxyaminomethylidene)-indan-1,3-dione align themselves antiparallel with each other in canted stacks parallel to the *a*-axis (Fig. 3). Intermolecular hydrogen bonding

Table 7
Hydrogen bonding contact distances (Å) in the crystal structure of 2-(hydroxyaminomethylidene)-indan-1,3-dione

Intermolecular contact distances	
N1···$O1_a$	3.17(1)
N1···$O3_c$	3.09(1)
H7···$O1_a$	2.45(1)
H6···$O3_c$	2.50(1)
N1···$O2_b$	3.04(1)
O1···$O2_d$	2.83(1)
H7···$O2_b$	2.44(1)
H5···$O2_d$	2.32(9)
Intramolecular contact distances	
N1···O2	2.94(1)
H6···O2	2.32(1)
H7···O1	2.38(1)
O1···O3	2.70(1)
H5···O3	1.90(10)

Estimated standard deviations are given in parentheses. Symmetry relationships: $a=1-x, -y, 1-z$, $b=1-x, 0.5-y, 1.5-z$, $c=x, 0.5-y, 0.5+z$, $d=x, 0.5-y, z-0.5$.

between stacks stabilizes the three dimensional structure with N–H···O=C, N–H···O–H and O–H···O=C intermolecular hydrogen bonding contacts observed (Table 7). Intramolecular hydrogen bonds are seen between N1–H6···O2 and O1–H5···O3. An analysis of the structural parameters in hydrogen bonded systems **A**–H···**B**, where **A** and **B** are the heavy atoms that are involved in hydrogen bonding, is crucial for understanding the decrease in the proton transfer barrier. According to the classification of nearly linear hydrogen bonds [21] (angle AHB is $>165°$), very low proton transfer barriers occur when the **A**···**B** distance is <2.5 Å (**A** and **B** are oxygen and/or nitrogen). The decreasing of the AHB angle usually leads to a reduction in the hydrogen bond energy. In the present case, the O1–H5–O3 angle is 140(8)° with an O1···O3 distance of 2.70(1) Å, suggesting only slow intramolecular proton transfer in the solid state. In the case of an **A**···**B** distance between 2.8 and 3.0 Å, the value of the proton transfer barrier is rather high.

4. Conclusions

Quantum-chemical calculations and NMR data indicate that two tautomeric forms, 2-(hydroxyaminomethylidene)-indan-1,3-dione and 2-carboamide-1-hydroxy-3-oxo-indan, are likely to coexist in the gas phase and in solution, with fast intramolecular proton transfer between them. In the solid state, X-ray crystallographic results suggest that 2-(hydroxyaminomethylidene)-indan-1,3-dione is the preferred tautomer.

Acknowledgements

The authors are indebted to Dr Mark Light at the EPSRC national crystallography service at the University of Southampton, UK for X-ray data collection. We (V.E. and S.A.) thank Prof. K. Davarsky, Bourgas University, for help with computing facilities.

References

[1] V.V. Moiseev, I.T. Poluektov, Usp. Khim. 42 (1973) 471.
[2] V. Enchev, Chem. Papers 48 (1994) 219.
[3] V. Enchev, Sn. Bakalova, G. Ivanova, N. Stoyanov, Chem. Phys. Lett. 314 (1999) 234.
[4] A. Ahmedova, V. Mantareva, V. Enchev, M. Mitewa, Int. J. Cosm. Sci. 24 (2002) 103.
[5] J.D. Korp, I. Bernal, T.L. Lemke, Acta Crystallogr. B36 (1980) 428.
[6] R.L. Horton, K.C. Murdock, J. Org. Chem. 25 (1960) 938.
[7] A.A. Granovsky, www.http://classic.chem.msu.su/gran/gamess/index.html.
[8] M.W. Schmidt, K.K. Baldridge, J.A. Boatz, S.T. Elbert, M.S. Gordon, J.H. Jensen, S. Koseki, N. Matsunaga, K.A. Nguyen, S. Su, T.L. Windus, M. Dupuis, J.A. Montgomery Jr., J. Comput. Chem. 14 (1993) 1347.
[9] J.B. Foresman, T.A. Keith, K.B. Wiberg, J. Snoonian, M.J. Frisch, J. Phys. Chem. 100 (1996) 16098.
[10] M.J. Frisch, G.W. Trucks, H.B. Schlegel, G.E. Scuseria, M.A. Robb, J.R. Cheeseman, J.A. Montgomery Jr., T. Vreven, K.N. Kudin, J.C. Burant, J.M. Millam, S.S. Iyengar, J. Tomasi, V. Barone, B. Mennucci, M. Cossi, G. Scalmani, N. Rega, G.A. Petersson, H. Nakatsuji, M. Hada, M. Ehara, K. Toyota, R. Fukuda, J. Hasegawa, M. Ishida, T. Nakajima, Y. Honda, O. Kitao, H. Nakai, M. Klene, X. Li, J.E. Knox, H.P. Hratchian, J.B. Cross, C. Adamo, J. Jaramillo, R. Gomperts, R.E. Stratmann, O. Yazyev, A.J. Austin, R. Cammi, C. Pomelli, J.W. Ochterski, P.Y. Ayala, K. Morokuma, G.A. Voth, P. Salvador, J.J. Dannenberg, V.G. Zakrzewski, S. Dapprich, A.D. Daniels, M.C. Strain, O. Farkas, D.K. Malick, A.D. Rabuck, K. Raghavachari, J.B. Foresman, J.V. Ortiz, Q. Cui, A.G. Baboul, S. Clifford, J. Cioslowski, B.B. Stefanov, G. Liu, A. Liashenko, P. Piskorz, I. Komaromi, R.L. Martin, D.J. Fox, T. Keith, M.A. Al-Laham, C.Y. Peng, A. Nanayakkara, M. Challacombe, P.M.W. Gill, B. Johnson, W. Chen, M.W. Wong, C. Gonzalez, J.A. Pople, GAUSSIAN 03, Revision B.04, Gaussian, Inc., Pittsburgh, PA, 2003.
[11] T. Helgaker, M. Jaszunski, K. Ruud, Chem. Rev. 99 (1999) 293.
[12] K. Wolinski, J.F. Hilton, P.J. Pulay, J. Am. Chem. Soc. 112 (1990) 8251.
[13] R. Hooft, Collect Data Collection and Processing User Interface: Collect: Data Collection Software, Bruker Nonius B.V., The Netherlands, 1998.
[14] Z. Otwinowski, Minor in methods in enzymology in: C.W. Carter, R.M. Sweet (Eds.),, Macromolecular Crystallography, Part A vol. 276, Academic Press, London, 1997, pp. 307–326.
[15] S. Mackay, C.J. Gilmore, C. Edwards, M. Tremayne, N. Stewart, K. Shankland, maXus: A Computer Program for the Solution and Refinement of Crystal Structures from Diffraction Data, Bruker Nonius B.V., The Netherlands, 1998.
[16] G.M. Sheldrick, SADABS ver. 2.10, Bruker AXS, Inc., Madison, WI, 2003.
[17] G.M. Sheldrick, SHELX97—Programs for Crystal Structure Analysis (Release 97-2), Institüt für Anorganische Chemie der Universität, Tammanstrasse 4, D-3400 Göttingen, Germany, 1998.
[18] L.J. Farrugia, J. Appl. Crystallogr. 30 (1997) 565.
[19] A.L. Speck, Acta Crystallogr. A46 (1990) C34.
[20] L.J. Farrugia, J. Appl. Crystallogr. 32 (1999) 837.
[21] W.W. Cleland, M.M. Kreevoy, Science 264 (1994) 1887.